Research Article

Haris Nubli, Jung Min Sohn*, and SangJin Kim

Determination of cryogenic temperature loads for finite-element model of LNG bunkering ship under LNG release accident

https://doi.org/10.1515/cls-2022-0205
received November 09, 2022; accepted June 28, 2023

Abstract: The rising demand for liquefied natural gas (LNG)-fueled ships requires the LNG bunkering facility that partially uses a ship-to-ship operation. The bunkering process of LNG fuel may have a greater risk due to LNG volatility. The cryogenic temperature of LNG poses a threat to the personnel and structural embrittlement to ships. Therefore, cryogenic spill protection optimization was introduced concerning the structural strength analysis using finite element (FE) by utilizing cryogenic temperature loads provided by the computational fluid dynamics (CFD) model of an LNG release. This study aims to build a platform for transferring the temperature load profile from CFD to FE software accurately. The CFD model usually uses a structured Cartesian grid, and the FE method adopts an unstructured tetrahedral or hexahedral mesh. As a result, both configurations store results at different positions, and it is not preferred for the load profile to be transferred directly. The error will be greater due to the variance of positions. Random Forest, a machine learning method, has been employed that uses a regression technique to deal with a continuous variable. An accurate load profile for the FE model can be obtained by adopting decision tree learning in Random Forest. The procedure for determining the temperature load profile is presented in this article.

Keywords: cryogenic temperature, LNG bunkering ship, machine learning, computational fluid dynamics, finite-element model

1 Introduction

In order to control air pollutant emission, the International Maritime Organization has established several emission control area that restricts ships with excessive exhaust gas of SO_X and NO_X. To deal with the new regulation, either many ships are being converted to operate on liquefied natural gas (LNG) as well as 303 new LNG-fueled ships are being commissioned since 2020 [1]. In consequence, the demand for LNG fuel increase to 3.01 million per year for the shipping sector use only [2]. Besides this, the LNG supply facility will be required in the major port to serve those LNG-fueled ships. A ship-to-ship platform such as an LNG bunkering ship is preferable, that it only requires a few land acquisitions and stores large quantities of LNG fuel rather than the truck-to-ship operation [3].

The European Commission reported that since 1986, there have been a significant number of LNG release accidents involving the loading/unloading, storing, and distribution, which are the bunkering activities [4]. The SAFEDOR risk model also included the LNG release during loading/unloading as a generic accident category for ships carrying LNG, besides collision and grounding [5]. The risks of this cryogenic release would impact both personnel and ship structures, such as cryogenic burn and steel embrittlement, respectively, since LNG is stored at −163°C [6]. Direct contact of LNG flow to a structure can rapidly cool the steel below the embrittlement temperature. Consequently, it would interfere with safety measures, including early detection, isolation, and blowdown, which might not be able to overcome the cryogenic hazard completely [7]. Further, the cryogenic flow could cause brittle cracks that ultimately cause the structure to collapse and escalate into a catastrophic disaster due to an initial event of LNG release [6,7].

* **Corresponding author: Jung Min Sohn,** Department of Marine Design Convergence Engineering, Pukyong National University, Busan, Republic of Korea; Department of Naval Architecture and Marine System Engineering, Pukyong National University, Busan, Republic of Korea, e-mail: jminz@pknu.ac.kr
Haris Nubli: Department of Marine Design Convergence Engineering, Pukyong National University, Busan, Republic of Korea
SangJin Kim: Department of Marine Environment and Engineering, National Sun Yat-sen University, Kaohsiung, Taiwan
ORCID: Jung Min Sohn 0000-0002-6495-479X

Based on those risk identification, a consequence analysis which is a part of risk assessment would be useful that provides a comprehensive analysis by conducting either experiment or simulation of an accidental LNG release [6,7]. The problem of LNG release simulation can be done by employing the turbulence flow model provided by the computational fluid dynamics (CFD) solver, *i.e.*, Kameleon Fire Ex (KFX) and flame acceleration simulator [8–10].

To deal with the cryogenic flow hazard, the cryogenic thermal and structural response must be performed to deliver an optimized structural design [6]. Lloyd Register published the cryogenic spill guidance that provides the cryogenic spill protection (CSP) procedure. Using CFD techniques, CSP requires identifying the most exposed area to a cryogenic hazard and predicts the cryogenic heat transfer to the structure in that area [7]. Furthermore, the result of cryogenic heat transfer in CFD analysis can be applied as an input for thermal-stress analysis using finite element (FE) [6,7]. By adopting this technique, the region of degraded material can be identified based on the cryogenic brittle fracture criterion. Thus, it would be useful to redesign the structure in case of brittle fracture escalation [7].

This study aims to build a platform for transferring the thermal data from CFD to FE software in order to support CSP assessment. The cryogenic gas leak model is based on an LNG bunkering ship's accidental release of LNG that was analyzed on KFX. The temperature in each coordinate point of the KFX grid was carried out as an input as well as the node information of the FE model, for Random Forest. *R*-squared and root mean square errors (RMSE) were employed to evaluate the Random Forest model. In addition, both temperatures in both KFX and FE models were compared to see the Random Forest accuracy. Finally, the temperature profile was obtained, which is compatible with the FE model's node position. This temperature profile is ready to use as input for further FE analysis.

2 Review of thermal load determination

The integration of load profiles derived from CFD into FE software for structural response analysis plays a crucial role in CSP assessment [6,7]. However, this integration task is challenging, as CFD and FE models often employ different mesh or grid configurations. While some commercial packages offer partial solutions, they are not fully compatible or versatile. For instance, FAHTS, designed for heat transfer analysis, can read radiation and convection from KFX simulation results but requires additional software, such as USFOS [11], to address the structural response problem [12]. Furthermore, the temperature profile cannot be exported to various FE software. Another limitation is that USFOS only supports FE models using beam elements for nonlinear structural response analysis.

To overcome these limitations, Kim *et al.* (2013) developed a platform called KFX2DYNA, specifically designed to map thermal loads from KFX to LS-DYNA for shell element problems [13]. This platform employs an interpolation technique to transfer the thermal load, with interpolation occurring at LS-DYNA nodes based on the closest KFX monitoring points [12,13]. Notably, popular FE software like ABAQUS also adopts interpolation for load transfer [14]. Alternatively, adopting an ensemble learning method, such as Random Forest, holds promise for load transfer. By constructing multiple decision

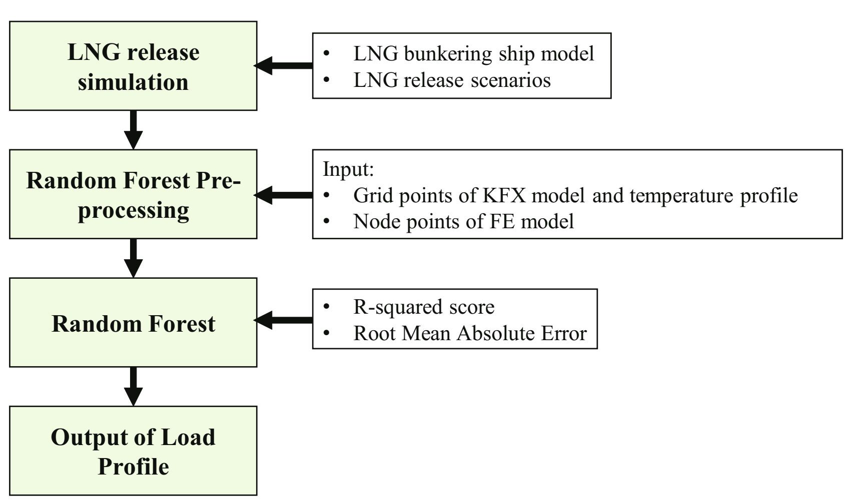

Figure 1: The framework of temperature load transfer.

trees in the training model, this technique can effectively address regression tasks, estimating the value of a target variable based on input variables [15]. Figure 1 provides an overview of the framework used to map temperature loads from KFX to FE models. Temperature loads are obtained from LNG release simulations using KFX, focusing on the LNG bunkering ship as the target model. Various LNG release scenarios are considered, encompassing parameters such as leak diameter, position, flow rate, wind speed, wind direction, and ambient temperature. The KFX simulation results, specifically the steel temperature, are retrieved from the area of interest for Random Forest pre-processing.

In this study, the Random Forest technique is employed to integrate KFX grid points, FE node positions, and the steel temperature output from KFX simulations. The positions of grid points and nodes are treated as dependent variables, with their values depending on the corresponding temperature values, which serve as the independent variable. Decision trees in the Random Forest model are constructed using KFX grid points and temperature load data. The FE node positions are then used as input to predict the temperature load. To evaluate the accuracy of the predictions, the R-squared score is employed, which measures the deviation between the predicted temperatures and the temperatures obtained from KFX simulations, taking into account the shape of the data. Additionally, the RMSE is used to assess the error in the data values, providing further insights into the performance of the Random Forest regression model. These evaluation techniques are commonly employed for assessing the efficacy of Random Forest regression models. Furthermore, a direct comparison of the load profiles between the KFX and FE models is performed at specific coordinate points, allowing for a comprehensive evaluation of the load transfer process and the fidelity of the predicted temperature load in the FE model.

3 The past study of LNG release

KFX is a CFD program based on the finite-volume model that uses a structured Cartesian grid to solve the conservation equations for three-dimensional time-dependent turbulent flow [6,8,9,16]. Several experimental data have been employed for validating the accuracy of the KFX code that focuses on the large-scale hydrocarbon release experiment [9,17,18]. In this study, an accidental LNG release occurred on the deck of the LNG bunkering system that was released from a point on a pipeline. The release duration was limited to 15 s following the response time of the emergency shutdown valve that was installed on the LNG bunkering system [19]. The detail of the LNG release scenario is given in Table 1.

Table 1: LNG release scenario for KFX simulation [20]

Leakage parameter	Variable (unit)
Hole diameter	50.00 mm
Leak flow rate	3.32 kg/s
Leak direction	To ship's stern
Leak duration	15.00 s
Environment parameter	**Variable (unit)**
Wind direction	From the ship's starboard
Wind speed	2.00 m/s
Ambient temperature	14.59°C

Figure 2 exhibits the gas cloud dispersion after the KFX simulation has been conducted. The contour is presented based on the lower flammability of LNG, which is a 5% gas concentration of the overall gas mixture. The LNG gas cloud was flown to the ship's stern that directly hit an obstruction which is a fuel gas supply room. Thus, this fuel gas supply room is an area of interest where a potential brittle crack may occur. The wall of the fuel gas supply room was significantly exposed to the gas cloud that has a temperature of up to 174.08 K or −99.07°C [19]. In this case, the gas release path was re-entrained after the gas cloud particles were reflected due to an existing nearby obstruction. The gas cloud dispersion decelerates because of the gas re-entrainment mechanism, which causes a gas cloud accumulation.

4 Load transfer process

This section addresses transferring the load profile from the CFD results to the FE model. The primary challenge stems from the disparity in mesh configurations between the two numerical models. To tackle this issue, a technique named Random Forest regression was employed, which offers a promising solution.

4.1 Pre-processing

In KFX, the result of various calculations is stored inside the control volume (CV) point such as fluid density and temperature, which is a scalar variable. The scalar variable is located in the middle of the CV, and the vector variable is

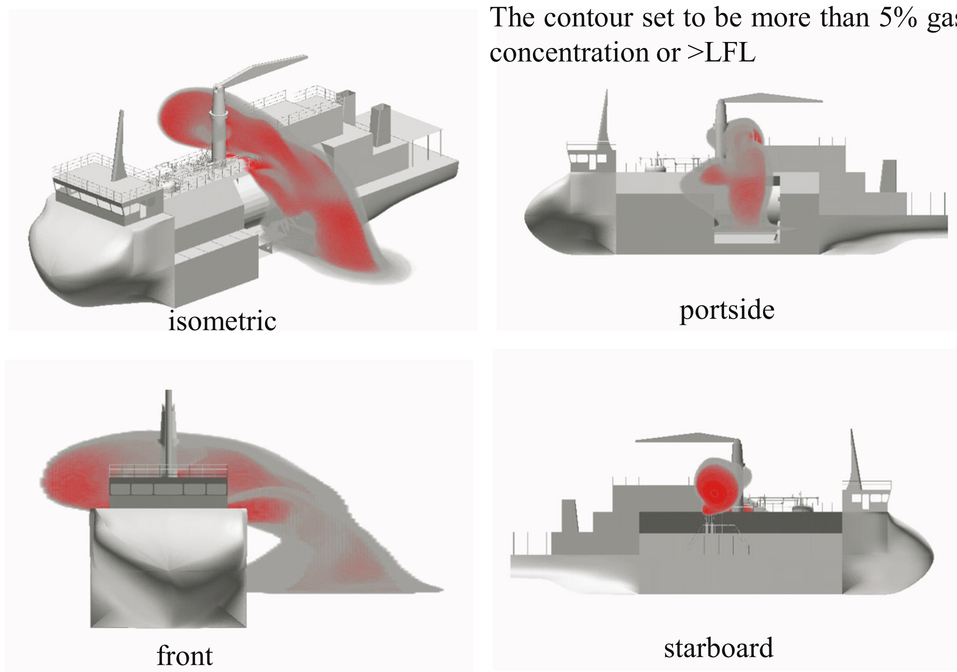

Figure 2: Gas cloud dispersion of LNG release simulation.

stored at the CV's boundary [16]. A non-uniform structured cartesian grid (NSCG) is adopted in KFX to solve the finite-difference problems [16]. Grids can be controlled to have different sizes of CVs, and the finer CV is used in the area of interest. The simulation process can be optimized in terms of result accuracy and simulation time with this grid control [16]. Figure 3 shows the NSCG configuration in KFX.

A different configuration is used in FE, which is adopting a non-uniform unstructured mesh. This mesh configuration can accommodate an arbitrary geometry [21]. Load information, such as forces, moments, and temperatures, can be stored inside a node point in the FE model [22]. Figure 4 exhibits an FE model of an LNG bunkering ship in ANSYS/LS-DYNA.

Grid and node points provide the position information in the Cartesian system. Thus, the independent variable consists of the coordinate point in the X, Y, and Z axes. It is followed by temperature profiles as the dependent

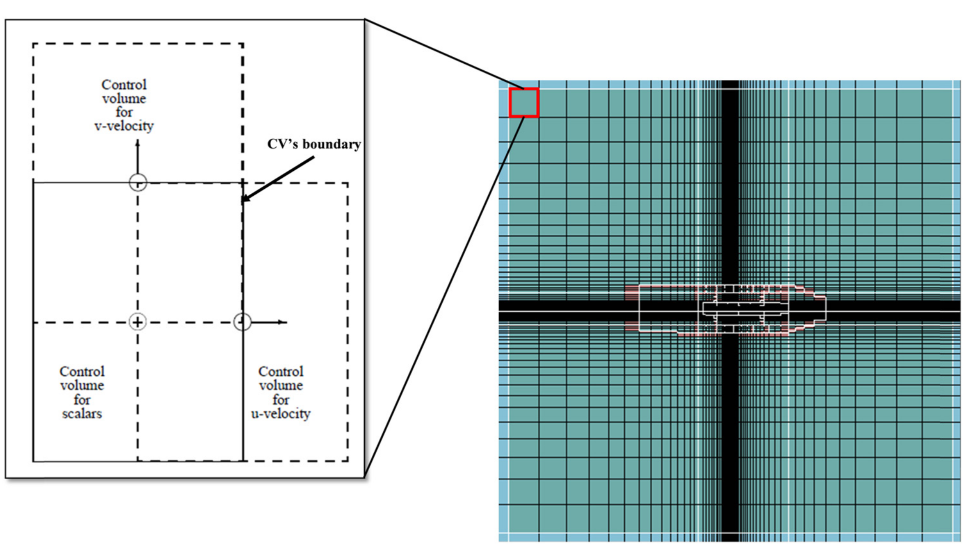

Figure 3: NSCG on KFX [16] with LNG bunkering ship model.

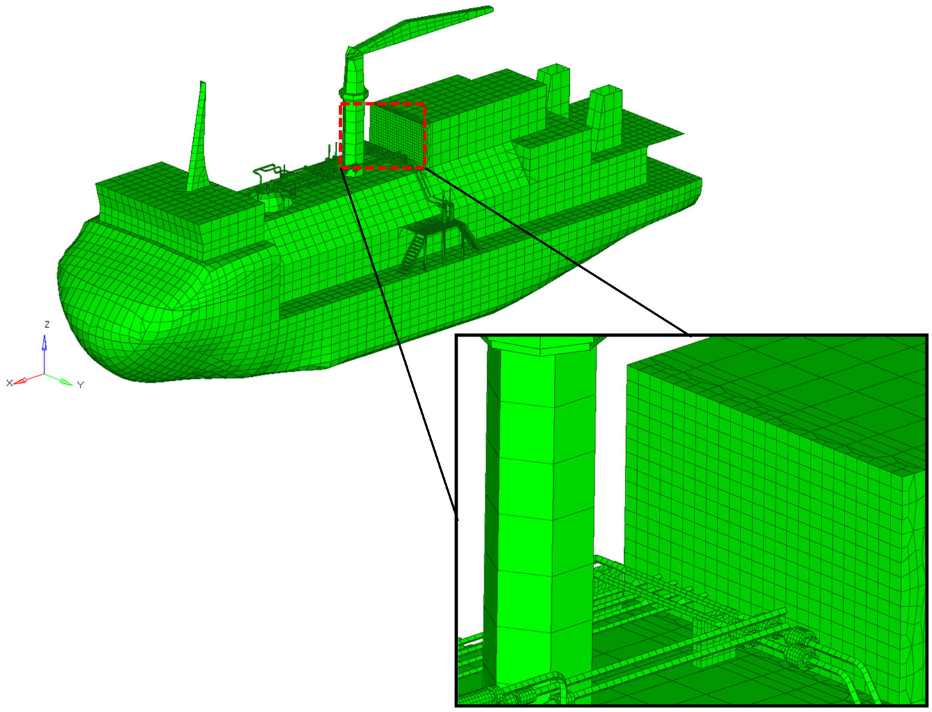

Figure 4: Non-uniform unstructured quadrilateral mesh used in ANSYS/LS-DYNA.

Table 2: Example of the input dataset

No.	Independent variable ("*X*")			Dependent variable ("*Y*")
	***X* (m)**	***Y* (m)**	***Z* (m)**	**Steel temperature (K)**
1	7.74	−0.60	10.15	149.18
2	7.95	−0.60	10.15	163.92
3	7.74	−0.70	10.15	217.11
4	7.95	−0.70	10.15	223.81
5	7.74	−0.50	10.15	229.56
6	7.95	−0.50	10.15	235.73
7	7.25	−0.60	10.05	241.08
8	7.25	−0.60	10.25	243.04
9	7.51	−0.60	10.05	250.28
10	7.51	−0.60	10.25	251.98

variable. The steel temperature is the only independent variable that was retrieved from the KFX result. Here is an example of the dataset for building a random forest model that was retrieved from KFX, as shown in Table 2. This dataset is limited to ten instances from the actual 29,865 instances.

4.2 Random forest procedure

This study implemented all the algorithms required for constructing the Random Forest model using Python code. The machine learning package "scikit-learn" was utilized to develop the algorithm [23]. The Random Forest model leverages decision trees to make predictions of the dependent variables based on the provided independent variables. Additionally, the study applied a technique known as "bagging" (bootstrapping–aggregating) to the Random Forest model. Bootstrapping involves randomly sampling the dataset with replacement to determine the values used in executing the decision tree algorithm [24,25]. Typically, 100 decision trees are employed to obtain precise results. The aggregation step involves selecting the majority of the data processed by the decision trees algorithm. In the case of regression problems, the decision tree results can be simply averaged to obtain the majority values [26]. Figures 5 and 6 exhibit the procedure for utilizing the Random Forest and an example of the bootstrapping–aggregating process, respectively.

Upon acquiring the KFX results, the dataset is categorized into grid points and corresponding steel temperatures. To develop the Random Forest model, the dataset is partitioned into training and testing subsets, constituting 80 and 20% of the entire dataset, respectively. The training subset plays a crucial role in identifying and learning the underlying data patterns within the Random Forest model [27,28]. Conversely, the testing subset is employed to assess the performance and progression of the Random Forest algorithm [27,29]. It is essential for the testing subset to represent the

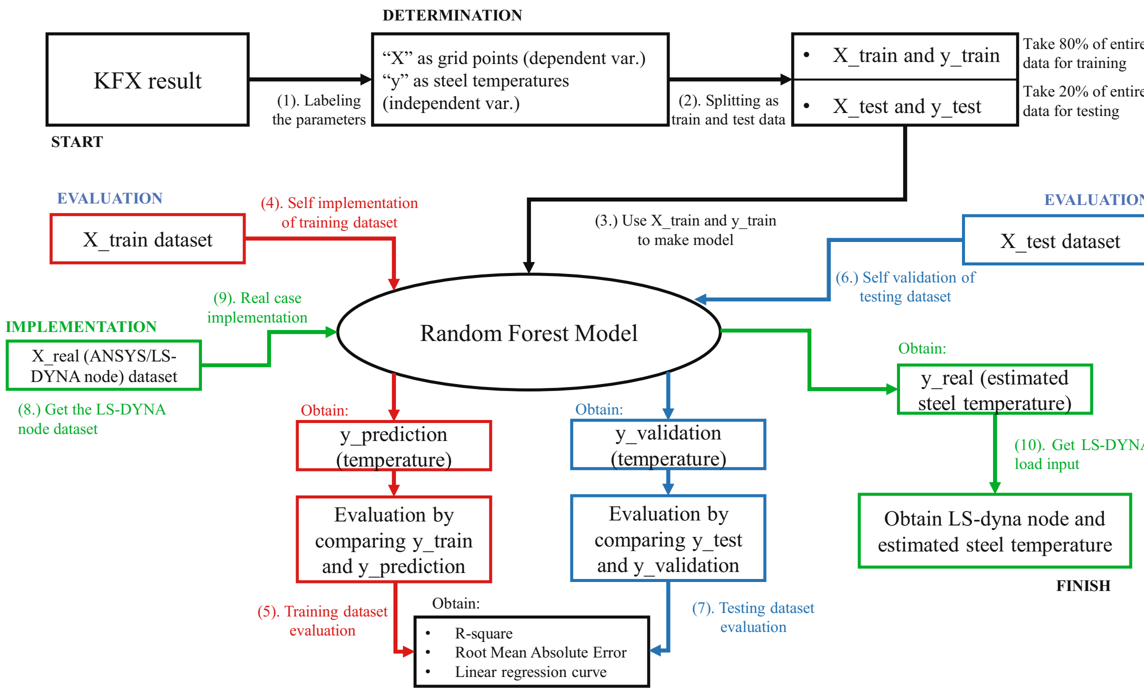

Figure 5: The framework of random forest.

Bagging:

Original dataset

No.	X (m)	Y (m)	Z (m)	Temperature (K)
1	16.82	1.05	11.00	254.72
2	16.82	1.16	11.11	259.33
3	16.49	1.16	11.90	260.64
4	16.49	1.16	12.20	269.13

Bootstrapping the dataset

No.	X (m)	Y (m)	Z (m)	Temperature (K)
1	16.82	1.05	11.00	254.72
2	16.82	1.16	11.11	259.33
3	16.49	1.16	11.90	260.64
3	16.49	1.16	11.90	260.64

With replacement

(a)

Aggregating:

A dataset with unknown temperature target

X (m)	Y (m)	Z (m)	Temperature (K)
16.826	1.058	11.008	?

No. of tree	Temperature (K)
1st	254.729
2nd	259.331
3rd	258.814
4th	255.879
Average	**257.188**

(b)

Figure 6: Bootstrapping (a) and Aggregating (b) process in Random Forest.

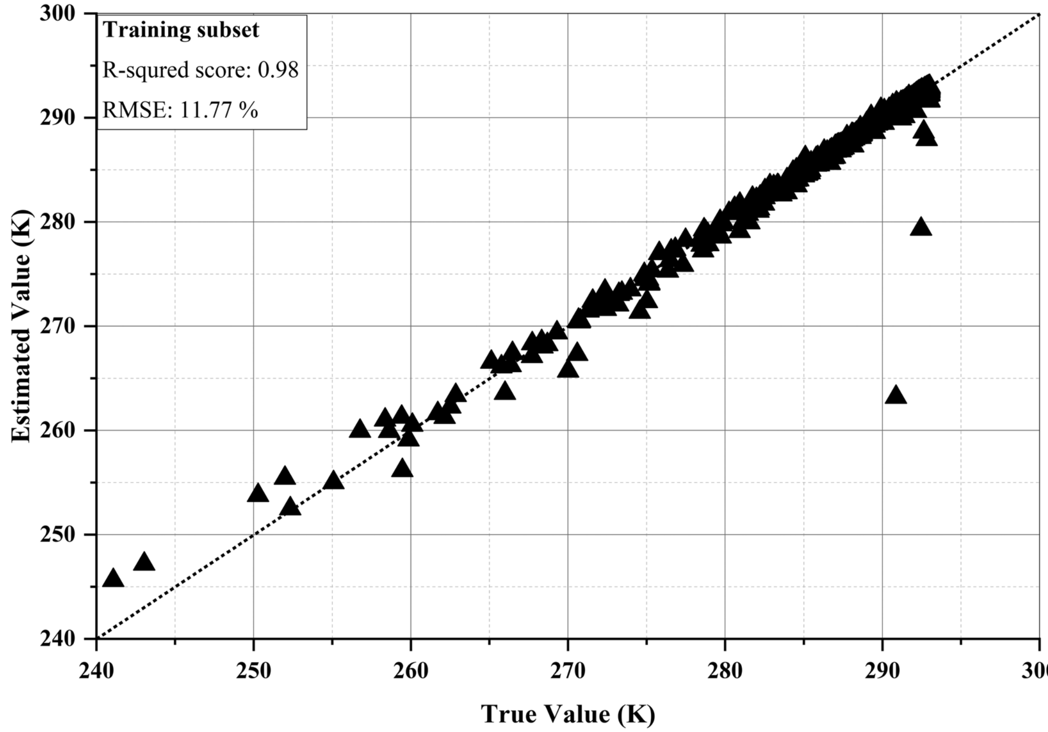

(a)

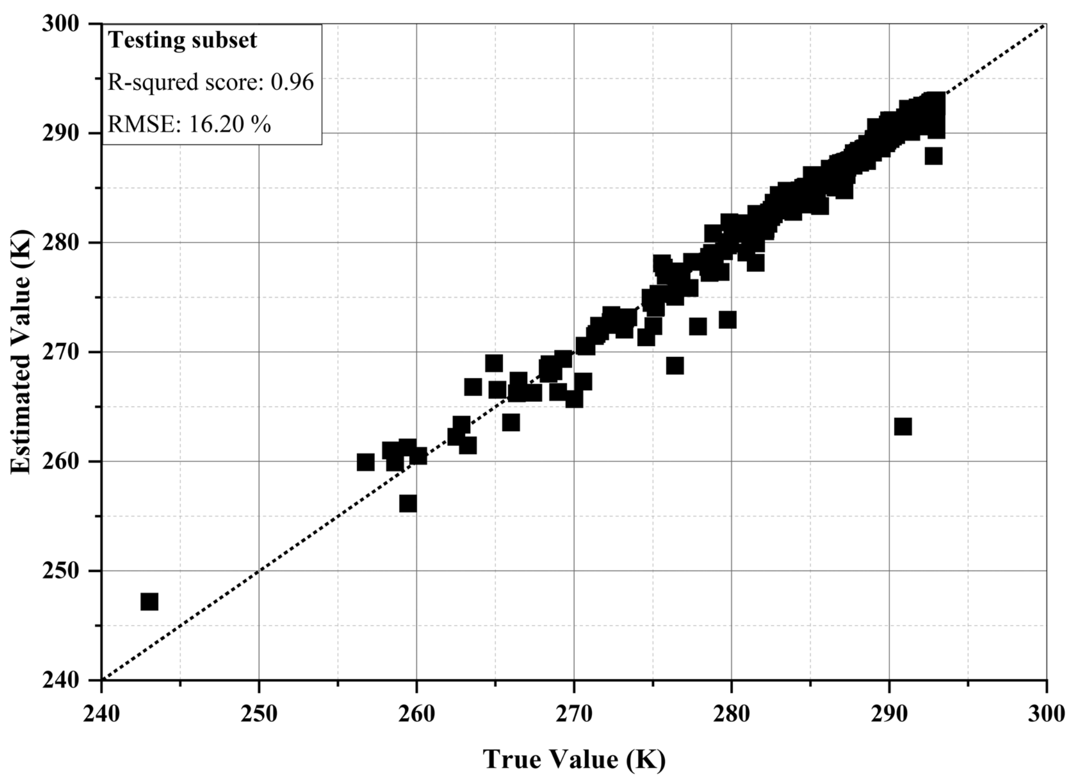

(b)

Figure 7: Plots of true and estimated steel temperatures; training (a) and testing subsets (b).

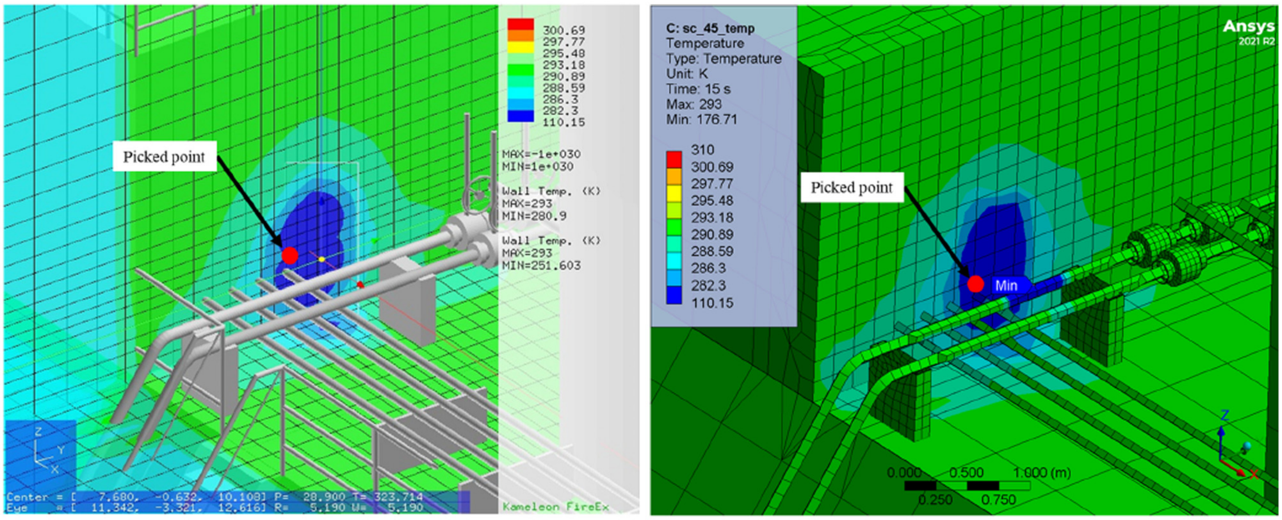

(a) (b)

Figure 8: The steel temperature plot of (a) KFX and (b) FE.

Table 3: Comparison of steel temperature between KFX and FE load profiles

Load profile	*X* (m)	*Y* (m)	*Z* (m)	Steel temperature (K)
FE	7.51	−0.60	9.50	284.15
KFX	7.50	−0.60	9.55	284.14
Discrepancy (%)				**0.002**

entire dataset adequately and possess sufficient data points to facilitate accurate predictions [27]. The training and testing subsets are vital components in the model development and evaluation process. An extensive evaluation was conducted to assess the performance of the Random Forest model by comparing the predicted values with the true values of the original dataset. Figure 7 presents the results of this evaluation, showcasing the plots alongside the corresponding R-squared score and root mean square errors. Here, the RMSE and R-squared score can be expressed as follows:

$$\mathrm{RMSE} = \sqrt{\frac{1}{n}\sum_i x_i^2}, \tag{1}$$

$$R^2 = 1 - \frac{\mathrm{RSS}}{\mathrm{TSS}}, \tag{2}$$

where n is the amount of the value, and x_i is each value which is steel temperature in this case. Furthermore, RSS and TSS are the sum of squares of residuals and the total sum of squares, respectively.

The training and testing subsets demonstrate a high R-squared score, indicating a strong correlation between the predicted and true values. The RMSE values are relatively low, further affirming the accuracy of the predictions. Notably, the training subset, comprising 80% of the entire dataset, exhibits a better fit than the testing subset. Overall, the evaluation outcomes indicate favorable results. During the implementation stage, the ANSYS/LS-DYNA node points (*X*_real) were utilized as the dependent variable. This variable plays a crucial role in estimating the new steel temperature data.

5 Load profile validation

To ensure the credibility of the load profile when applied in the FE software, an additional evaluation was conducted. Specifically, a comparison was made between the steel temperature datasets obtained from KFX and the Random Forest model. The temperature contours for both datasets were prepared using the same range of contour colors and are presented in Figure 8. In terms of the temperature contour, both plots exhibit a similar shape, primarily located on the wall of the fuel gas supply room. However, it is worth noting that certain equipment details were omitted in the FE model to focus on the structural analysis of the ship. As a result, there are variations in the sizes of the independent variables between the two models. To validate the consistency of the steel temperatures, two points were selected for comparison, situated in almost identical positions along the wall of the fuel gas supply room. Table 3 provides detailed information about these selected points.

The comparison between the steel temperatures obtained from KFX and the FE load profiles demonstrates a high level of agreement, as the discrepancies in temperature values are negligible. This agreement further reinforces the credibility of the load profile when utilized in the FE software, confirming the accuracy and reliability of the Random Forest model's predictions.

6 Conclusion

This article presents a platform for integrating load profiles obtained from CFD and FE models to facilitate CSP assessment. The proposed approach involves utilizing a Random Forest regression model to construct the temperature load profile for the FE model. Key aspects of the study include conducting CFD-based gas dispersion analysis for an LNG bunkering ship model and retrieving steel temperature results from KFX, along with grid points and FE node positions. The obtained dataset serves as input for the Random Forest model, which demonstrates good agreement between the *R*-squared score and RMSE during the evaluation stage. The implementation stage involves utilizing ANSYS/LS-DYNA node points to generate a suitable load profile for FE input, resulting in minor discrepancies between steel temperatures from KFX and FE models. The Random Forest model is a valuable alternative to interpolation techniques, offering a wider range of variables and ensuring coverage of all destination nodes without relying solely on the steel temperature value at the nearest nodes. Future studies will focus on conducting structural response analysis of the LNG bunkering ship, considering the effects of cryogenic temperature loads using FE simulations.

The proposed platform exhibits the potential of the Random Forest approach in integrating load profiles from different models, thereby contributing to the field of CSP assessment. By effectively combining CFD and FE data, the platform enables a comprehensive understanding of temperature load profiles for accurate risk assessment. This research provides valuable insights for the optimization of LNG bunkering operations, particularly in terms of safety considerations. The findings highlight the significance of considering cryogenic temperature loads and offer a practical and reliable tool for engineers and practitioners involved in the design and analysis of LNG bunkering structures.

Funding information: This research was supported by Korea Institute of Marine Science & Technology Promotion (KIMST) funded by the Ministry of Oceans and Fisheries (RS-2023-00255929). The first author also acknowledges the support by a grant from Brain Korea 21 Program for Leading Universities and Students (BK21 FOUR) MADEC Marine Designeering Education Research Group.

Author contributions: Conceptualization, J.-M.S. and H.N.; methodology, J.-M.S. and H.N.; software, H.N.; validation, H.N.; formal analysis, H.N.; investigation, J.-M.S. and H.N.; resources, J.-M.S. and S.-J.K.; data curation J.-M.S. and H.N.; writing – original draft preparation, H.N.; writing – review and editing, J.-M.S. and H.N.; visualization, H.N.; supervision, J.-M.S. and S.-J.K; project administration, J.-M.S.; funding acquisition, J.-M.S.

Conflict of interest: Authors state no conflict of interest.

References

[1] DNV AS. Alternative Fuel Insight. DNV; 2021. https://www.dnv.com/maritime/insights/topics/lng-as-marine-fuel/market-update.html.

[2] Le Fevre C. A review of demand prospects for LNG as a marine transport fuel. Oxford, United Kingdom: The Oxford Institute for Energy Studies; 2018. p. 35. doi: 10.26889/9781784671143.

[3] EMSA Guidance on LNG bunkering to port authorities and administrations. EMSA; 2018. https://safety4sea.com/wp-content/uploads/2018/02/EMSA-Guidance-on-LNG-Bunkering-to-Port-Authorities-and-Administrations-2018_02.pdf. [Accessed: 05/Nov/2022].

[4] European Commission. eMARS: Electronic major accident report system. European Commission; 2021. https://emars.jrc.ec.europa.eu/en/emars/content. [Accessed: 05/Nov/2022].

[5] Vanem E, Antão P, Østvik I, de Comas FDC. Analysing the risk of LNG carrier operations. Reliab Eng Syst Saf. 2008;93(9):1328–44.

[6] Pujol J, Kleiveland RN, Lileheie NI, Holmas T, Amdahl J. Advanced cryogenic structural collapse analysis CSCA - Part II: Cryogenic flow and structural cooling. Offshore Technology Conference Asia; 2016 Mar 22–25; Kuala Lumpur, Malaysia.

[7] Lloyd's Register. Guidance Notes for Risk Based Analyses. London, UK; Cryogenic Spill; 2015. https://www.lr.org/en/knowledge/lloyds-register-rules/guidance-notes/guidance-notes-for-risk-based-analysis-cryogenic-spill/. [Accessed: 21/Aug/2023].

[8] Magnussen BF. On the structure of turbulence and a generalized eddy dissipation concept for chemical reaction in turbulent flow. 19th Aerospace Sciences Meeting; 1981 Jan 12–15; St. Luis (MO), USA. AIAA, 1981.

[9] Rian KE, Grimsmo B, Lakså B, Vembe BE, Lilleheie NI, Brox E, et al. Advanced CO_2 dispersion simulation technology for improved CCS safety. Energy Procedia. 2014;63(1876):2596–609. doi: 10.1016/j.egypro.2014.11.282.

[10] Li XJ, Zhou RP, Konovessis D. CFD analysis of natural gas dispersion in engine room space based on multi-factor coupling. Ocean Eng. 2016;111:524–32. doi: 10.1016/j.oceaneng.2015.11.018.

[11] Kim JH. A new procedure for fire structural assessment of offshore installations [PhD dissertation]. Busan, South Korea: Pusan National University; 2014.

[12] Paik JK. Advanced structural safety studies. Topics in Safety, Risk, Reliability and Quality. Vol. 37. Singapore: Springer Nature Singapore; 2020.

[13] Kim SJ, Lee J, Kim SH, Seo JK, Kim BJ, Ha YC, et al. Nonlinear structural response in jet fire in association with the interaction between fire loads and time-variant geometry and material properties. Ocean Eng. 2017;144:118–34. doi: 10.1016/j.oceaneng.2017.08.028.

[14] Hibbitt D, Karlsson B, Sorensen P. Abaqus/CAE User's Guide. Providence (RI), USA: Dassault Systemes Simulia Corp; 2013. http://130.149.89.49:2080/v2016/books/usi/default.htm? startat = pt06ch58s06.html
[15] Opitz D, Maclin R. Popular ensemble methods: An empirical study. J Artif Intell Res. 1999;11:169–98. https://jair.org/index.php/jair/article/view/10239.
[16] Vembe BE, Rian KE, Holen J, Lilleheie NI, Grimsmo B. Kameleon FireEx 2000 (Theory Manual). Brisbane: ComputIT; 2001.
[17] Nubli H, Sohn JM. CFD-based simulation of accidental fuel release from LNG-fuelled ships. Ships Offshore Struct. 2020;17(2):1–20. doi: 10.1080/17445302.2020.1827806.
[18] Rian KE, Vembe BE, Evanger T. KFX™ Validation Handbook. Trondheim: ComputIT; 2016.
[19] Nubli H, Sohn JM, Jung D. Temperature reduction on LNG bunkering ship structure under accidental cryogenic gas release using CFD simulation. ASME 2022 41st International Conference on Ocean, Offshore and Arctic Engineering; 2022 Jun 5–10; Hamburg, Germany. ASME, 2022.
[20] Nubli H, Sohn J, Jung D. Consequence analysis of accidental LNG release on the collided structure of 500 cbm LNG bunkering ship. J Mar Sci Eng. 2022;10(10):1378. https://www.mdpi.com/2077-1312/10/10/1378.
[21] Manchester CFD. All there is to know about different mesh types in CFD! University of Manchester; 2021 [cited 2022 Jul 10]. https://www.manchestercfd.co.uk/post/all-there-is-to-know-about-different-mesh-types-in-cfd. [Accessed: 05/Nov/2022].
[22] ANSYS/LS-DYNA. User's manual for ANSYS/LS-DYNA. New York: ANSYS Inc; 2020.
[23] scikit-learn: Machine learning in python. scikit-learn; 2007 [cited 2022 Jul 11]. https://scikit-learn.org/stable/. [Accessed: 05/Nov/2022].
[24] Breiman L. Bagging predictors. Mach Learn. 1996;24(2):123–40. http://link.springer.com/10.1007/BF00058655.
[25] Rocca J. Ensemble methods: bagging, boosting and stacking. Towards Data Science; 2019 [cited 2022 Jul 11]. https://towardsdatascience.com/ensemble-methods-bagging-boosting-and-stacking-c9214a10a205.
[26] Breiman L. Random forest. Mach Learn. 2001;45(5):32. https://link.springer.com/article/10.1023/A:1010933404324.
[27] Barkved K. The difference between training data vs. test data in machine learning. obviously.ai; 2022 [cited 2022 Jul 11]. https://www.obviously.ai/post/the-difference-between-training-data-vs-test-data-in-machine-learning#:~:text = In machine learning%2C datasets are, known as the testing data. [Accessed: 05/Nov/2022].
[28] Zhang C, Ma Y. Ensemble machine learning: Methods and applications. New York (NY), USA: Springer New York; 2012. p. 1–329.
[29] Antariksa G, Muammar R, Lee J. Performance evaluation of machine learning-based classification with rock-physics analysis of geological lithofacies in Tarakan Basin, Indonesia. J Pet Sci Eng. 2022;208:109250. doi: 10.1016/j.petrol.2021.109250.